

GNNAnatomy: Systematic Generation and Evaluation of Multi-Level Explanations for Graph Neural Networks

Hsiao-Ying Lu, Yiran Li, Ujwal Pratap Krishna Kaluvakolanu Thyagarajan, Kwan-Liu Ma

Abstract— Graph Neural Networks (GNNs) have proven highly effective in various machine learning (ML) tasks involving graphs, such as node/graph classification and link prediction. However, explaining the decisions made by GNNs poses challenges because of the aggregated relational information based on graph structure, leading to complex data transformations. Existing methods for explaining GNNs often face limitations in systematically exploring diverse substructures and evaluating results in the absence of ground truths. To address this gap, we introduce GNNAnatomy, a model- and dataset-agnostic visual analytics system designed to facilitate the generation and evaluation of multi-level explanations for GNNs. In GNNAnatomy, we employ graphlets to elucidate GNN behavior in graph-level classification tasks. By analyzing the associations between GNN classifications and graphlet frequencies, we formulate hypothesized factual and counterfactual explanations. To validate a hypothesized graphlet explanation, we introduce two metrics: (1) the correlation between its frequency and the classification confidence, and (2) the change in classification confidence after removing this substructure from the original graph. To demonstrate the effectiveness of GNNAnatomy, we conduct case studies on both real-world and synthetic graph datasets from various domains. Additionally, we qualitatively compare GNNAnatomy with a state-of-the-art GNN explainer, demonstrating the utility and versatility of our design.

Index Terms—Graphlets, Motif, Graph Neural Network, Explainable AI, Visual Analytics, Visualization

1 INTRODUCTION

A Graph Neural Network (GNN) is a machine learning (ML) approach used to transform graphs into vector representations, which are more easily utilized in classification or prediction tasks involving graph data. For instance, consider a teamwork scenario represented as a network, where the participants are nodes and the collaboration between two individuals forms an edge. Each network can be labeled based on historical data indicating whether its outcome was successful or not. By learning the associations between the teamwork structure and outcomes, a GNN can predict the likelihood of success for future teamwork endeavors. To derive actionable insights, the ability to explain the behavior of GNNs is essential; for example, in the teamwork scenario, understanding the underlying reasons for an unsuccessful outcome becomes crucial to implementing interventions to avert the undesirable performance.

To unravel the black box of GNNs, existing explainable GNN approaches, such as [26, 33], typically focus on identifying crucial subgraphs that have the greatest influence on GNN behavior. However, besides investigating subgraphs, many real-world applications necessitate identifying the basic building blocks of a graph (i.e., elementary substructures or recurring patterns) and understanding the function and significance of each substructure. For instance, in biological networks, it is a 6-atom carbon ring that renders a molecule mutagenic [3], rather than a specific subgraph containing a 6-atom carbon ring. Furthermore, previous literature offers limited explorations for alternative explanations. Most methods generate a single subgraph or an ensemble of subgraphs as the explanation without seeking potential alternative explanations. Since such subgraph-level explanations do not always accurately explain the GNN behavior, it is imperative to enable the exploration of diverse substructures and also seek for substructure explanations to derive the most trustworthy explanations.

Another challenge lies in the granularity of explanations. Previous GNN explanation approaches generate either instance- or model-level explanations [36]. While instance-level explanations are tailored for individual graphs [33], they limit the overall understanding of GNN behavior. In response to this limitation, model-level explanations aim to interpret GNN behavior for the entire dataset or for graphs belonging to the same class [17, 31, 35]. However, it is often the case that more than one substructure contributes to making a graph distinguishable. For

example, the classification of a molecule’s mutagenicity involves both a 3-atom acyclic substructure, NO_2 , and a 6-atom carbon ring [3]. The NO_2 substructure alone can mark some graphs as mutagenic, whereas others require only the carbon ring or a combination of both traits for differentiation. Merely suggesting common substructures in a class fails to encompass these detailed explanations, and thus neither instance-level nor model-level explanations offer sufficient granularities [27]. The ability to identify groups of graphs that require different explanations and determine the most explanatory substructure for each group is thus crucial.

Validating explanations is not a trivial task due to the absence of ground truths regarding which substructures the GNN should be utilizing. Most evaluation metrics are based on the intuition that when explanatory nodes and links are removed from the original graph, there will be a significant change in the GNN prediction [8, 19]. However, removal-based methods pose risks for graph data, as removing a subgraph can often result in the new graphs being out-of-distribution (OOD) compared to the original graphs [7, 14, 18, 29]. Moreover, metric scores are typically used for comparative purposes among different GNN explainers instead of assessing potential explanations to determine the best one. A systematic evaluation method is required to examine the relevance of generated explanatory substructures.

Given these limitations and remaining challenges, we present novel methods aimed at addressing each of them within the context of graph-level classification tasks.

- To generate substructure explanations, we employ *graphlets* as explanatory elements. Each graph is represented as a vector composed of graphlet frequencies, facilitating a simpler neighboring data space directly derived from the original graphs. This approach offers a summary of basic substructures for each graph, and is not only to better facilitate explanation but also applicable to any graphs. Subsequently, we approximate the GNN performance using the graphlet frequency vectors.
- To provide granular GNN explanations, we identify groups of graphs that require different classification rules by illustrating the relationships between GNN classifications and graphlet frequencies. By specifying groups of graphs for which explanations are generated, we address the absence of group-level explanations.
- To ensure reliable evaluation and explore potential alternative explanations, we derive two metrics from factual and counterfactual reasoning processes to systematically assess the relevance of each graphlet as a potential explanatory substructure.
- With our methods, we introduce GNNAnatomy, a visual analytics

• All authors are with University of California, Davis. E-mail: {hyllu, ranli, ujwkal, klma}@ucdavis.edu.

system designed to support interactive generation and evaluation of substructure explanations at the needed granularities.

2 BACKGROUND

This work employs graphlets to explain the behavior of graph neural networks in graph-level classification tasks. In this section, we offer concise background information on the two techniques.

2.1 Graphlets and Graphlet Frequencies

Graphlets are small connected non-isomorphic graphs [4, 20]. Given a specific number of nodes in a graphlet, there is a fixed number of graphlet types. For example, we show all 6 graphlet types with 4 nodes in Fig. 1. Graphlets have been used in both analysis and visualization of graphs and networks [12, 25].

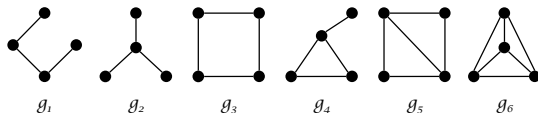


Fig. 1: Six graphlet types with four nodes.

The relative frequencies of different graphlet types can be used to characterize the topology of a graph. For the 6 graphlet types g_1, g_2, \dots, g_6 in Fig. 1, a 6D vector of graphlet frequencies \mathbf{f}_G is extracted to represent the graphlet distribution in each graph G :

$$\mathbf{f}_G = (f_{g_1}, f_{g_2}, \dots, f_{g_6}), \quad (1)$$

where

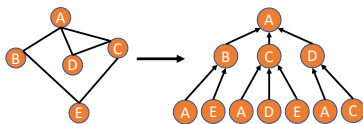
$$f_{g_k} = \frac{\#(g_k \subseteq G)}{\sum_{i=1}^6 \#(g_i \subseteq G)}. \quad (2)$$

In the actual computation of graphlet frequencies, it is too time-consuming to count the exact occurrence of each graphlet $\#(g_i \subseteq G)$ because comparing all possible connected subgraphs is an NP-hard problem. Therefore, we adopt the connected subgraph sampling method in [23], and compute the frequency of each type of graphlet among a set of subgraphs (with 3, 4, and 5 nodes) sampled from G . For any graph G , we concatenate the 2D vector of the 3-node graphlet frequencies, the 6D vector of the 4-node graphlet frequencies, and the 21D vector of the 5-node graphlet frequencies into a single 29D graphlet representation.

2.2 Graph Neural Networks

Graph Neural Networks (GNNs) are machine learning models designed to operate on graph-structured data, allowing them to extract relational characteristics inherent in graphs. As depicted in Fig. 2, in a GNN, each node undergoes a series of operations across multiple layers. Take node A for instance, in the first layer l_1 , the GNN aggregates messages from the direct neighbors of node A (i.e., nodes B, C , and D). It then combines this aggregated message with the node representation of A from the previous layer l_0 to update the node representation of A in layer l_1 . This process repeats for every node in each subsequent layer, l_N , where $N = 1, 2$ in this example. The learned node representations/embeddings serve as structural features for performing various downstream tasks in GNNs, including node classification, edge prediction, or graph classification. In node classification tasks, the node representations are utilized as input to a classifier, enabling the prediction of the respective node labels. In graph classification tasks, the embeddings of all nodes are aggregated into a single graph embedding, which serves as input to the downstream classifier for predicting the overall graph label.

Fig. 2: GNN aggregate information from layers of neighbors. The right side shows a 2-layer neighbor hierarchy for learning node A embedding.



3 RELATED WORKS

The field of explainable graph neural networks (GNNs) is still in its early stages of development, with relatively few works exploring this area. Nonetheless, inspired by the success in explaining computer vision models, researchers have approached explainable GNNs from various angles. In this sections, we provide an overview of previous approaches and remaining limitations and challenges. Subsequently, we discuss visual analytics works contributing to explaining GNNs. Finally, we review common metrics used for evaluating GNN explanations.

3.1 Subgraph Explanations

Existing GNN explanation works strive to elucidate GNN performance by pinpointing a subgraph that significantly influences GNN classifications or predictions. Perturbation-based methods, such as those introduced in [6, 22, 28, 33, 37], utilize generators trained to produce masks (e.g., node or edge masks) applied as perturbations to input graphs. The objective is to perturb graphs in a manner that retains important structural information, thus preserving similar GNN predictions as the original graphs. However, these approaches often face potential biases due to the soft masks, which yield continuous values between 0 and 1, making the generated explanations challenging to interpret. Conversely, surrogate-based methods [9, 26, 34, 38] leverage interpretable surrogate models to approximate GNN predictions using local neighboring data derived from input graphs. Despite their interpretability, defining neighboring data for graphs presents a challenge. The neighboring space should be simpler to comprehend and representative of the original discrete graphs, which contain structural information. Consequently, finding such neighboring data for graphs is non-trivial. Nevertheless, these methods typically yield a specific subgraph as an explanation, whereas in practice, there is often a need to identify the general substructure that influences GNN behavior. For instance, it is more useful to ascertain that it is the ring structure causing a molecule to be mutagenic, rather than merely identifying a subgraph containing a ring as the explanation. Furthermore, constrained by the design of generating subgraph explanations, previous literature has limited exploration into potential alternative explanations. There may exist subgraphs with similar topologies to the explanation that are not adequately justified as to why they are less important than the explanatory subgraph. In essence, it is vital to provide substructure explanations rather than subgraph explanations and allow for the exploration of diverse substructures before determining the most explanatory one.

3.2 Instance/Model-Level Explanations

A taxonomic survey conducted by Yuan et al. [36] categorizes GNN explanation methods as either model-level, which elucidates the global behavior of GNNs, or instance-level, which produces explanations specific to each graph instance. While the majority of existing GNN explanation works focus on interpreting why GNNs make predictions or classifications for individual graph instances, as introduced in Sec. 3.1, instance explanations alone are insufficient to provide a comprehensive understanding of GNN behavior. Given the multitude of graph instances in a training dataset, deriving a global understanding from individual instance explanations is not feasible. In contrast, several model-level methods have been proposed. To name a few, Xuanyuan et al. [31] treat neurons in GNNs as individual concept detectors capable of interpretation and generalization across multiple instances. PGExplainer [17] learns a parameterized model to rate the importance of each edge in the input space. XGNN [35] learns a graph generator that provides a set of graphs maximizing a target prediction, containing distinct vital graph patterns relevant to the global behavior of GNNs. However, while most existing model-level methods aim to interpret GNN behavior across entire datasets or graphs from the same class, they often lack granularity. For example, in the classification of a molecule’s mutagenicity, while a 6-atom carbon ring alone may indicate mutagenicity in some graphs, others may require the presence of NO_2 as well. This renders neither instance-level nor model-level explanations sufficient. Therefore, to achieve flexible granularity in explanations, it is crucial to identify groups of graphs that require different explanations and determine the valid explanatory substructure for each.

3.3 Visual Analytics for Explaining GNNs

According to a recent survey [13], there has been little visual analytics effort in explainable GNNs. We discuss several methods dedicated to GNN model evaluation, diagnosis, and domain-specific interpretations. Liu et al. [15] proposed an interactive system that connects node embeddings with both the topological neighborhood and node features for model evaluation. Additionally, GNNLens [10] was developed to explain and diagnose prediction results using metrics and correlations between an instance and its neighbors. However, the topological correlations and metrics developed in these works consider only the 1-hop neighbors and focus on explaining the predictions of nodes in a graph. Wang et al. [27] designed a drug repurposing visual analytics system, which uses GraphMask [22] to extract critical meta-paths understandable by domain experts. Similar to our concerns, this work also highlights the need for domain experts to generate explanations for GNNs at needed granularities. Nonetheless, their visualization design choices largely depend on domain preferences, which hinders their applicability to other graph datasets and GNN architectures.

3.4 GNN Explanation Evaluation Metrics

Evaluations are necessary to ensure the validity of the generated explanations. Some metrics, such as accuracy (F1 or ROC-AUC scores) [21, 33], require ground truth motifs for computation and are often used to evaluate explanations for synthesized graph datasets. Fidelity [8, 19] refers to the concept that well-suited explanations, if removed, will change GNN predictions. Sparsity [19] pertains to the idea that explanations should be compact and minimally affect the node size and edge density of the original graph when removed. Building upon these two measuring concepts, various metrics can be derived [1, 16]. Yet, when evaluating the fidelity of a generated explanatory substructure, removal-based methods often encounter issues with out-of-distribution (OOD) scenarios [7, 14, 18, 29]. Despite efforts to mitigate the OOD problem with emerging generation-based approaches, they still suffer from biases and deviations from the original model behavior [5, 30]. Some other works evaluate their explanations based on the reasoning process, distinguishing between factual and counterfactual explanations. Factual explanations are deemed *sufficient* substructures that lead to the same prediction, while counterfactual explanations are regarded as *necessary* substructures that, once removed, alter the prediction. Commonly derived metrics include probabilities of sufficiency and necessity [2, 24]. Sufficiency measures the percentage of graphs whose factual explanation substructures alone maintain GNN predictions, while necessity measures the percentage of graphs whose counterfactual explanation substructures, if removed, change GNN predictions. Still, there is no standard format for evaluating GNN explanations and addressing additional issues such as OOD and model behavior deviations.

4 METHODOLOGY

As outlined in Sec. 3, existing explainable GNN methods encounter limitations in terms of (1) explorativity, (2) granularity, and (3) evaluability. This section describes how we address these challenges.

4.1 Graphlet Frequency: Topological Summary

Given the fundamental role of elucidating graph structures in GNNs, as opposed to explicating node/edge features, which is more aligned with methodologies for non-graph data, this work places emphasis on discerning the importance of substructures.

As outlined in Sec. 2.1, our method utilizes connected non-isomorphic small graphs, or graphlets, as the foundational elements for constructing GNN explanations. By calculating the frequency of each graphlet within a graph, we derive a topological summary represented as a vector. This summarization is achieved through the use of k -node graphlets, specifically for $k = 3, 4, 5$. To illustrate with $k = 5$ as an example, we extract 5-node connected subgraphs from the original graph employing the efficient sampling method detailed in [23]. For each of these sampled subgraphs, we determine their isomorphism to each of the 21 distinct 5-node graphlets. The frequency of each 5-node

graphlet within the graph is quantified by the ratio of isomorphic instances to the total sampled subgraphs. This procedure is similarly applied for $k = 3$ and $k = 4$, enabling a comprehensive topological characterization across different graphlet sizes. Ultimately, we compile a 29-dimensional (29D) vector by concatenating the 2D, 6D, and 21D topological summaries derived from the frequencies of the 3-, 4-, and 5-node graphlets, respectively.

Leveraging graphlets as the foundational elements for explanations enhances explainable GNN methodologies in several ways: Firstly, the process of topological summarization is universally applicable to any graph data. Given that current GNN explanations frequently take the form of subgraphs, as reviewed in Sec. 3.1, establishing a consistent framework for constructing explanations is beneficial. This uniformity ensures a unique mapping between explanatory substructures and generated explanations, preventing evaluation difficulties arising from slight structural variances. Secondly, the utilization of graphlets as explanatory tools is inherently intuitive due to their compact size. This simplicity makes it easier to understand and differentiate each substructure from other graphlets, facilitating clearer and more straightforward explanations. Lastly, explanations derived from graphlets provide insights into the general substructures that GNN models potentially leverage for making predictions. Existing methods tend to pinpoint a specific subgraph within the original graph as the key contributor influencing GNN predictions. However, in many datasets, it is the substructures that play a pivotal role in shaping the behavior of GNNs, rather than any specific segment of the graph. For instance, it is the 6-atom carbon ring structure causing a molecule graph to be mutagenic, rather than a specific subgraph containing a carbon ring. Our approach extracts the general substructure patterns that GNNs consider important, offering a more generalized understanding of what drives model predictions.

4.2 Graph Neural Network: Graph-level Classification

Our approach utilizes graphlets to provide intuitive substructure explanations for GNNs within graph-level classification tasks. Graph-level classification tasks involve GNNs predicting the probability distribution across potential classes for the label of a graph. This means that the GNN model assesses an entire graph as an input and outputs a prediction regarding which category or class the graph belongs to, based on learned structural traits within the graph data. The typical approach involves the GNN first learning to generate a comprehensive embedding for each graph. This embedding encapsulates the essential structural information of the graph. Subsequently, this graph embedding is used as input to a simple linear layer, which serves to reduce the dimensionality of the embedding down to the number of potential classes. The application of a softmax function on this output then yields a probability distribution, where each probability lies between 0 and 1, and the sum of all these probabilities equals 1. The rationale behind employing a simple linear layer for dimensionality reduction of graph embeddings to probabilities is founded on the premise that if the GNN has effectively learned the embedding, it should retain ample structural information from the input graph to facilitate accurate predictions. Therefore, a simple linear transformation suffices for this critical step, translating the rich, learned embeddings into understandable class probabilities.

We adhere to this conventional approach to train our GNN models, ensuring not only accurate classification probabilities but also the preservation of crucial topological characteristics within the graph embeddings. We train a Graph Convolutional Network (GCN) [11] on graph classification tasks using both real-world and synthetic datasets. Prioritizing the aggregation of structural information, we discard any node or edge attributes, opting instead for the one-hot encoding of node degrees as the initial vector for each node. Our GCN architecture consists of four layers, followed by a fully connected layer. The outputs of the four hidden layers, each with a dimensionality of 20, are concatenated to form node embeddings, which are then aggregated into an 80-dimensional graph embedding. The decision to utilize 4-layer architecture is closely tied to our utilization of graphlets. Given that the largest diameter among graphlets is 4 (specifically, the 5-node acyclic graphlet), it becomes necessary to employ up to 4 layers in our GNNs. This enables the models to aggregate information from nodes up to 4

hops away and effectively capture up to 5-node substructures within the graph. Furthermore, by concatenating the output from each hidden layer to form the graph embeddings, we facilitate the expression of substructures captured from lower-hop neighbors in the graph embeddings. This helps mitigate any preferential bias towards the 5-node structures, which would potentially dominate in the last layer of the network. Thus, our approach ensures a more balanced representation of the various substructures within the graph.

4.3 Surrogate Model: GNN Performance Approximation

To improve the interpretability of our explanations, we propose the use of surrogate models designed to approximate the behavior of GNNs by leveraging simpler neighboring data derived from input graphs. Specifically, we develop a machine learning (ML) encoder-decoder architecture aimed at reconstructing the graph embeddings produced by GNNs based on the graphlet frequency vectors. Notably, although the use of connected graphlets to approximate GNN behavior may not capture disconnected topological information, if present, this approximation aligns with the aggregation mechanism of GNNs, which gather information from direct neighbors.

For each graph, we utilize its 29-dimensional graphlet frequency vector as input to the *encoder*. Through two 20-dimensional hidden layers, the *encoder* outputs a 10-dimensional bottleneck latent vector. This 10-dimensional latent vector is then fed into a linear layer and softmax function, reducing the dimensionality from 10 to 2D probabilities. The *encoder* is supervised by the probability outputs produced by a trained GCN using L2 loss, aiming to reconstruct the GCN’s performance. The *decoder* takes the 10-dimensional latent vector as input. Through two 20-dimensional hidden layers with symmetrical residual connections from the *encoder*, it outputs an 80-dimensional reconstructed graph embedding. This reconstructed graph embedding is then fed to the frozen classification model trained alongside our GCN, transferring the 80-dimensional embeddings to 2-dimensional softmax probabilities. The training of the *decoder* is guided by two loss functions: the graph embedding reconstruction loss and the probability reconstruction loss (i.e., mean squared error/L2 loss).

We train our encoder-decoder model by alternating between training the *encoder* and the *decoder*. Specifically, we train the *encoder* for one step and then freeze its weights to obtain the latent vector, which is fed into the *decoder*. After updating the *decoder* weights for one step, we freeze its weights and commence the next training step for the *encoder*. This training scheme ensures that the *encoder* generates latent vectors that preserve similar structural information as the GCN. These latent vectors can then be reconstructed into similar graph embeddings, resulting in similar classification probabilities. Moreover, our architecture inherently mitigates the possibility of overfitting. By reducing the graphlet information to a 10-dimensional latent vector in the *encoder*, we create a bottleneck that forces the model to learn a compact and general structural representation, which enables successful reconstruction in the *decoder*. This bottleneck also prevents the model from simply memorizing the mapping between graphlet frequency vectors and graph embeddings because most raw graphlet information (i.e., input of *encoder*) is substantially reduced.

Furthermore, our approach addresses the challenge of defining a suitable neighboring data space for graphs as discussed in Sec. 3.1. By extracting graphlet frequencies directly from the original graphs, we ensure that these frequencies accurately represent the neighboring space relative to the original data. Moreover, existing methods mostly focus on identifying local neighboring graphs. In contrast, the graphlet frequency vector acts as a comprehensive structural summary of each graph, applicable across various graph types. Therefore, our method for constructing a neighboring space is not confined to local representations but extends to a global scale, enhancing the overall comprehensiveness.

4.4 Factual and Counterfactual Explanation Evaluation

To explore diverse graphlet substructures and formulate hypothesized explanations, we have developed a visual analytics system, elaborated upon in detail in Sec. 5. Through examining relationships between GNN classifications and graphlet frequencies, users select a specific

graphlet as their hypothesized explanation. Subsequently, we employ two reasoning processes—factual and counterfactual—to assess the validity of this explanation. For instance, if the hypothesized explanation is *graphlet*₂, it must sufficiently contribute to the GNN’s ability to maintain its current classifications to be deemed successful in the factual reasoning process. To quantify this sufficiency, we employ Spearman’s correlation coefficient. Specifically, we analyze the correlation between the GNN classification confidence scores and the frequency of *graphlet*₂ across all graphs of interest to the user. This correlation coefficient indicates the extent to which the frequency of *graphlet*₂ aligns with the trend observed in the GNN’s classification probabilities. A high correlation coefficient suggests that the presence or absence of *graphlet*₂ significantly influences the GNN’s classifications, supporting its role as a meaningful factual explanatory factor.

A successful counterfactual explanation necessitates demonstrating its indispensability for a GNN to preserve its current classifications. This implies that the removal of the explanatory graphlet should significantly alter the GNN’s classification confidence. To remove a substructure from the original graph, we introduce perturbations in the graphlet frequency vector as input to our surrogate models, as described in Sec. 4.3. We then observe how these perturbations influence the classification results. Specifically, we conduct two inference runs for each graph using the trained surrogate model. The first run employs the original, non-perturbed graphlet frequency vector as input, obtaining the classification confidence from the surrogate model. Given that the surrogate model only approximates the GNN’s behavior, this initial run is crucial for establishing baseline comparison standards. The second run involves inputting the perturbed graphlet frequency vector to assess its impact on the surrogate model’s classification confidence. Perturbation involves setting the frequency of the targeted graphlet to zero.

To accurately account for the interdependencies among graphlets of varying sizes, such as between 4-node and 5-node graphlets, our method carefully considers the hierarchical nature of these substructures. For example, a 4-node star graphlet is a subgraph of a 5-node star graphlet. This relationship necessitates adjustments in their frequencies during perturbations. Consider the case where the perturbation targets a 4-node star graphlet. Upon setting its frequency to zero, it is imperative to adjust the frequency of any containing graphlet, such as the 5-node star, to zero as well. Conversely, when targeting a 5-node star graphlet for perturbation (i.e., set the frequency of the 5-node star graphlet to zero), adjustments are required for the frequency not only of the 4-node star graphlet but also of other 4-node graphlets interdependent on the 5-node star. This adjustment is necessary because a 5-node star can be formed by adding edge(s) and node(s) to any dependent 4-node graphlet. To compute this adjustment, we utilize a softmax function on the frequencies of the dependent 4-node graphlets. This function produces a softmaxed frequency vector, providing an estimate of how much each 4-node dependent graphlet contributes to the formation of the 5-node star graphlet. Subsequently, for each dependent 4-node graphlet, we subtract from it the frequency of the 5-node star graphlet weighted by its softmaxed frequency. This adjustment process is applied across all interdependent graphlets, retrieving and calibrating the frequencies of the dependent graphlets from 5-node to 4-node, and recursively from 4-node to 3-node graphlets.

After introducing perturbations (i.e., target graphlet removal) to the graphlet frequency vector, we compare the classification confidence before and after the removal by calculating the sum of the absolute values of L1 distance for each graph between the two inference runs. A high L1 distance indicates that the selected graphlet serves as a critical substructure, substantially influencing the GNN’s classifications. Additionally, we utilize the confidence scores output by the complete encoder-decoder model to initially project the graphlet frequency vector to the same graph embedding space as the GCN. This approach mitigates the influences stemming from performance differences between the surrogate model and the GCN when computing the L1 distance between the two confidence scores. Furthermore, our strategy of perturbing the original graphs through adjustments to their graphlet frequency vectors, coupled with the identification of graphlet interdependencies,

addresses the out-of-distribution (OOD) challenge. The OOD issue arises when the removal of a subgraph leads the residual structure to deviate from the original graph’s distribution, often resulting in inaccurate classifications due to these off-manifold inputs. Employing the original graph’s structural summary (i.e., the graphlet frequency vector) as a baseline for comparison ensures consistent behavior from the surrogate model. By considering the interdependencies between graphlets during perturbation, we enhance the perturbed graphs’ realism.

5 VISUAL ANALYTICS OF GNNANATOMY

Our visual analytics system stands as a pivotal tool for the interactive development and assessment of explanations. By employing graphlets as the explanatory elements, the evaluation metrics extend beyond comparing different explanation methods to include an examination of each substructure’s contribution to GNN classifications. Typically, existing explainers utilize a common metric for evaluation, establishing a baseline to identify the most effective method according to the metric used. Yet, this approach lacks indicators to inform users whether the baseline itself is sufficiently robust. Addressing this gap, our system integrates an additional validation layer into the explanation formulation process. This enables users to scrutinize all substructures, assessing their relevance to GNN classifications and determining their potential as explanatory factors through both quantitative and qualitative visual aids provided by our visual analytics system.

The system consists of four columns that facilitate the workflow of GNNAnatomy. Firstly, in the *Graph Group Selection* column, the *projection map* visualizes the relationship between graphlet frequencies and GNN classifications, aiding users in identifying a group of graphs of interest. Secondly, the *Substructure Explanatory Ranking* column assists in creating an explanatory hypothesis by providing class-wise *graphlet distribution* for each graphlet. Next, in the *Explanatory Substructure Evaluation* column, the validity of the hypothesis can be assessed through the support from *fidelity scatterplots*, which offer both visual and quantitative insights into the sufficiency and necessity of the hypothesis. Finally, to demonstrate the overall impact of substructures on the graph topology, two network visualizations are provided in the *Substructure Impact on Overall Topology* column. Notably, in this interface, the classification probability output for the class a graph belongs to is referred to as “confidence”. Conversely, the classification probability output for $Class_1$ is termed as “classification probability”. For instance, in a Discussion graph (i.e., $Class_0$), if the GCN probability output is $[0.75, 0.25]$, its confidence score is 0.75 and the classification probability is 0.25. In the following paragraphs, we will introduce these visual components in detail, highlighting the specific information they convey.

5.1 Graph Group Selection

As depicted in Fig. 3(a), this column comprises three components. Firstly, a slider is incorporated to enable users to filter the graphs based on their confidence scores. Users can choose the group of graphs with higher or lower confidence scores than the slider value through the dropdown menu in Fig. 3(a1). The remaining graphs are projected onto a scatterplot, as shown in Fig. 3(a2). This projection map helps users discern the associations between graphlet frequency vectors and graph embeddings by projecting them from high-dimensional space to a single value. The x-axis value of each graph represents the first principal component (PC1) of its graphlet frequency vector (i.e., graphlet frequency projection), while the y-axis value encodes the PC1 of the graph embedding generated by the GNN (i.e., graph embedding projection). In this scatterplot, users can lasso-select a group of graphs for which explanations are generated, highlighted with outlined pink and blue. To further refine the selection, the chosen group of graphs is redrawn into two histograms, as illustrated in Fig. 3(a3). Each histogram displays the graph distribution over confidence scores, empowering users to select specific sections of confidence scores for different classes through brushing. By providing connections between GCN classifications and graphlet frequencies, this column enables the creation and assessment of GNN explanations at specified levels of granularity.

5.2 Substructure Explanatory Ranking

As depicted in Fig. 3(b), a sequence of histograms presents the class-wise distributions of graphs within the selected group across the frequencies of each graphlet. The ranking (i.e., the order of display from top to bottom) of graphlets is determined by either our factual or counterfactual metric, based on the chosen explanation mode from the dropdown menu. As elaborated in Sec. 4.4, our factual metric sorts graphlets by the descending absolute value of Spearman’s correlation coefficient, while the counterfactual metric ranks graphlets based on the descending sum of absolute L1 distances between the confidence scores from original and perturbed graphs. Hovering over any bin within a histogram automatically highlights all bins of the same class across all histograms by increasing their opacity, providing a clearer visual representation of the distribution. This visual component guides users towards potential explanations for the GNN behavior of the selected group of graphs. Upon clicking a graphlet, users can evaluate the validity of this graphlet in detail.

5.3 Explanatory Substructure Evaluation

As depicted in Fig. 3(c), we offer two fidelity visualizations: factual and counterfactual fidelity scatterplots.

Factual explanation fidelity. In Fig. 3(c1), a scatterplot is presented, where each graph in the selected group is plotted with its frequency of the chosen graphlet encoded as the x-axis value and the classification probability encoded as the y-axis value. This scatterplot enables users to inspect the alignment between graphlet frequency trends and classification probabilities, indicating the efficacy of the graphlet in explaining GNN behavior for classifying the selected group of graphs. Quantitatively, the Spearman’s correlation coefficient, displayed in the top right corner, provides a statistical measure of this relationship. This visualization updates only when users choose “factual” via the explanation mode dropdown menu in Fig. 3(b).

Counterfactual explanation fidelity. In Fig. 3(c2), two scatterplots illustrate class-wise L1 distances between confidence scores derived from two surrogate model inferences using original and perturbed graphs, as explained in Sec. 4.4. These scatterplots provide detailed insights into changes in classification confidence, distinguishing between positive (improved confidence due to graphlet removal) and negative (decreased confidence due to graphlet removal) effects for each graph, symbolized by triangles along the y-axis. The x-axis denotes the frequencies of the selected graphlet in the original graphs. Additionally, a summation of absolute L1 distances is displayed in the upper right corner, serving as a summary of confidence changes resulting from perturbations (i.e., graphlet removal).

5.4 Substructure Impact on Overall Topology

As illustrated in Fig. 3(d), two network visualizations serve as examples to depict the overall topological impact resulting from differences in the frequency of the chosen graphlet. In the factual explanation mode, the **top view** (i.e., Fig. 3(d1)) showcases the structure of the graph with the lowest frequency of the selected graphlet. This graph is selected from the class with generally lower frequencies of the chosen graphlet. For instance, if there’s a negative correlation between the graphlet frequency and the classification probability, the class with lower frequencies of the selected graphlet is $class_1$. Conversely, the **bottom view** (i.e., Fig. 3(d2)) displays the graph with the highest frequency of the selected graphlet from the class with generally higher frequencies. In the case of a negative correlation, this graph would be from $class_0$.

In the counterfactual explanation mode, the **top view** shows the network with the smallest change in classification confidence following a perturbation, while the **bottom view** presents the graph experiencing the largest change in classification confidence after perturbation. By comparing the structures of representative graphs, users can map the impact from substructures to overall topologies, enabling them to reason about the typical appearance of graphs from different classes.

6 CASE STUDIES

We demonstrate the capabilities of GNNAnatomy through case studies using both real-world and synthetic graph datasets. Alongside quanti-

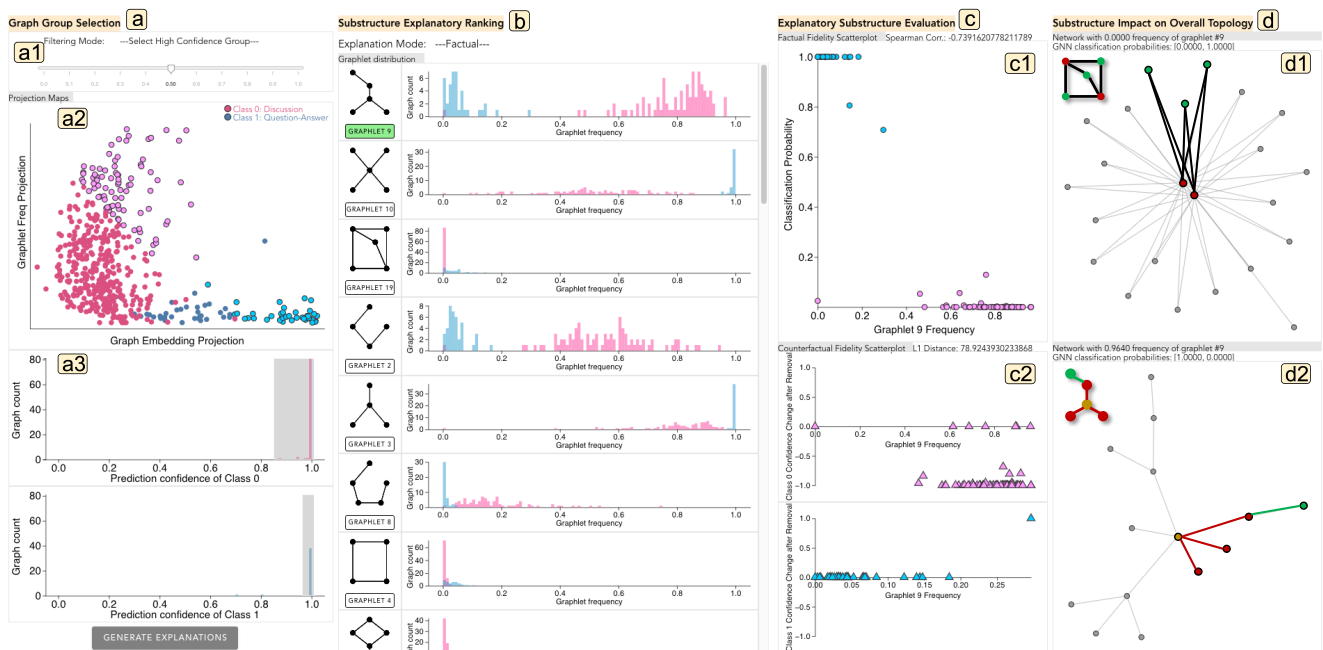


Fig. 3: This screenshot showcases the GNNAnatomy interface, designed for generating and evaluating explanations regarding GNN behavior on a selected group of graphs from the Reddit-Binary dataset. Users begin by selecting the groups of graphs for which explanations will be generated in (a). In (a1), users can filter graphs based on their classification confidence scores, using a slider bar. In this example, we opt to analyze graphs with classification confidence scores higher than 0.5. (a2) displays the remaining graphs, highlighting those selected with a lasso tool outlined in pink and blue. Further refinement of the graph selection is possible in (a3). Upon clicking the "GENERATE EXPLANATIONS" button, examination shifts to view (b). Here, users can choose between two explanation modes: factual and counterfactual, via a dropdown menu. In each mode, the explanatory ranking of graphlets is determined by the corresponding metric, evaluating their relevance to GNN classifications. For each graphlet, a class-specific bar chart presents the distribution of graphs based on its frequency. Users can click on any graphlet to verify its potential explanation validity in (c). In this instance, *graphlet₉* is selected, and (c1) displays the correlation between the frequency of *graphlet₉* and the classification probability of the two classes. (c2) illustrates the changes in classification confidence scores of each graph in the selected group after *graphlet₉* removal. Finally, (d) depicts the impact of the chosen substructure, *graphlet₉*. (d1) and (d2) highlight the typical graph topologies of the two classes.

tatively measuring the validity of the graphlet explanations using our factual and counterfactual metrics, we compare our explanations to those generated by GNNExplainer [33]. We opted to compare with GNNExplainer because it (1) identified important motifs for datasets lacking ground truths and (2) its explanatory subgraphs have been widely utilized as baselines for comparison with most other explainers. The quantitative evaluation metric proposed by GNNExplainer focuses on a specific subgraph’s alignment with the ground truth, which isn’t suitable for the substructure explanations generated by GNNAnatomy. Therefore, we provide qualitative comparisons between GNNAnatomy and GNNExplainer’s explanations.

6.1 Datasets

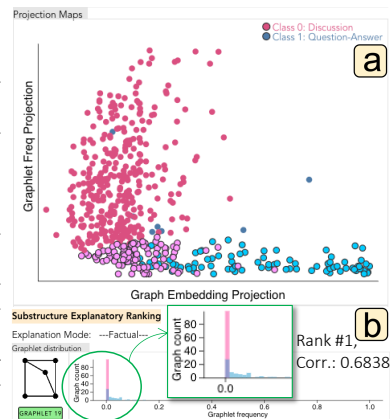
6.1.1 Real-World Datasets

We utilize two real-world graph-level binary classification datasets. **Reddit-Binary** [32] comprises 2000 graphs, each representing a discussion thread extracted from Reddit. In these graphs, nodes correspond to users engaging in the thread, while edges denote replies between users’ comments. The graphs are labeled based on the nature of user interactions observed in the threads. Specifically, the dataset distinguishes between two types of interactions: Question-Answer, extracted from the subreddits *r/IAmA* and *r/AskReddit*, and Discussion, logged from the subreddits *r/TrollXChromosomes* and *r/atheism*. **Mutagenicity** [3] consists of 4337 molecule graphs, each labeled based on its mutagenic effect on the Gram-negative bacterium *S. typhimurium*.

6.1.2 Synthetic Dataset

To construct a graph dataset with ground truth motifs, we draw inspiration from the approach proposed by Ying et al. [33]. They utilized the Barabasi-Albert random graph model (BA) to generate a base graph comprising 300 nodes. This base graph was then enriched by attaching 80 house motifs. The task for GNN is to perform node classifications across four classes: nodes within the top, middle, and bottom sections

Fig. 4: (a) illustrates the selection of a group of graphs with similar topologies, aimed at observing subtle substructural differences between the two classes in Reddit-Binary dataset. (b) indicates the top-ranked factual explanatory graphlet and the graph distribution over its frequency. The correlation coefficient reflects the strong relationship between its frequency and the classification probability.



of a house motif, along with nodes in the base graph itself. Given that our explainer aims to elucidate GNN behavior in graph-level classification tasks, we create **BA-House** with graph labels. We employ the BA model to generate 300 base graphs, each with a random node count ranging from 10 to 40. Subsequently, for half of these base graphs, we attach a random number of house motifs, ranging from 2 to 10. The ratio between the size of a base graph and the number of attached house motifs maintains consistency with the ratio used in [33] (i.e., 300 nodes in the base graph and 80 attached house motifs). These 300 synthesized graphs are then labeled with two classes: those without any attached house motifs and those with attached house motifs. Given the design of the dataset, it is hypothesized that the primary substructure crucial for GNN classifications would be the attached motif, namely, the house substructure.

6.2 Study 1: Reddit-Binary

Experiment settings. We train the GCN and surrogate model using graphs with fewer than 100 nodes due to the computational cost associated with graphlet frequency calculation. Among the remaining 554 graphs, consisting of 101 graphs of the Question-Answer (QA) class and 453 graphs of the Discussion class, the GCN model achieves a classification accuracy of 0.9549 (i.e., over 0.5 confidence score), while the classification probabilities output by the surrogate model exhibit a cosine similarity of 0.9322 with the GCN probabilities output.

Group-level explanations. As depicted in Fig. 3(a2), the projection map reveals that Discussion graphs display a more diverse range of structural characteristics, as their graphlet frequency projections are scattered along the y-axis. In contrast, the graphlet frequency projections of Question-Answer (QA) graphs remain tightly clustered at the bottom of the y-axis, indicating a more consistent topology among QA graphs. Most graphs from different classes are separable along the x-axis (i.e., graph embedding projection), indicating that the GCN has successfully captured distinguishable structural features even for those graphs at the bottom with similar topologies across classes. We further explore the potential substructures that contribute to the GCN’s ability to make such classifications.

We choose a group of graphs with distinct topologies and graph embeddings (i.e., separated graphlet frequency projections and graph embedding projections) as shown in Fig. 3(a2). This selection aims to identify the salient substructure differences between the two classes that are relevant to the behavior of the GCN. In Fig. 3(b), the distribution of the top-ranked graphlet, *graphlet₉*, in the factual explanation mode exhibits clear separation across classes. This suggests that classifying graphs based solely on the frequency of *graphlet₉* could potentially achieve the same high classification accuracy as the GCN, which is 0.9549. The factual fidelity scatterplot, depicted in Fig. 3(c1), validates a strong negative correlation (Spearman correlation corr.: -0.74) between the frequency of *graphlet₉* and the classification probability. Furthermore, in Fig. 3(c2), the necessity of *graphlet₉* in maintaining the current GCN classifications is confirmed. Upon removal of *graphlet₉*, the confidence scores of Discussion graphs decrease while those of QA graphs with unusually high frequencies of *graphlet₉* increase. These changes indicate that the GCN tends to classify most graphs as QA graphs when *graphlet₉* is absent from their topologies, thereby validating the explanatory power of *graphlet₉*. In Fig. 3(d1, d2), the visualizations of graphs with the lowest and highest frequencies of *graphlet₉* communicates the topological traits of the two classes: QA graphs (Fig. 3(d1)) tend to have multiple centralized individuals that interact with most others, whereas Discussion graphs (Fig. 3(d2)) typically feature branched-out discussions. Annotations in Fig. 3(d2) and the context of the Reddit-binary dataset indicate that *graphlet₉* captures common branched-out discussions, absent in typical QA graphs (Fig. 3(d1)).

Further examination of the projection map prompts us to investigate another set of graphs, as shown in Fig. 4(a). While the GCN model generally distinguishes between graphs from different classes, they appear scattered along the x-axis. This scattering occurs because some Discussion graphs share similar topologies with QA graphs at the bottom of the y-axis. As a result, capturing the salient structural differences might not be enough for the GCN to make effective classifications, and it is pushed to uncover subtle topological disparities between classes. These subtle structural differences are encoded in the graph embeddings learned by GCN, which further scatter the projections of graphs from each class within their respective clusters. Consequently, we focus on selecting graphs with similar topologies to identify these subtle structural disparities that aid in the GCN’s classification effectiveness. As depicted in Fig. 4(b), the frequency of the top-ranked *graphlet₁₉* correlates with the GCN classification probability with a correlation coefficient of 0.6838. Additionally, the typical topological trait of QA graphs observed in the previous group of graphs is encapsulated by *graphlet₁₉*, as annotated in Fig. 3(d1). This suggests a reasoning process for the GCN: while the common structural trait of Discussion graphs (*graphlet₉*) is sufficient to distinguish most graphs, when classifying graphs with similar topologies, the common structural trait of

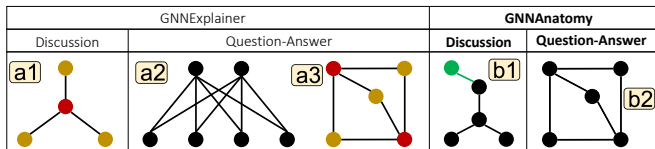


Fig. 5: (a1, a2) represent the ground truth motifs of each class in the Reddit-Binary dataset proposed by GNNExplainer. (a3) depicts the translation of (a2) to the graphlet setting. (b1, b2) showcase the extracted explanatory graphlet substructures of each class in Reddit-Binary by GNNAnatomy.

QA graphs becomes the next indicator that the GCN relies on.

In summary, it is evident that GCN employs different substructures to classify separate groups of graphs. GNNAnatomy not only helps users identify these groups but also rank the relevance of graphlets using on our factual and counterfactual metrics. By interactively evaluating the potential explanations, users can formulate a satisfactory explanatory substructure for the chosen group.

Qualitative evaluation. As depicted in Fig. 5(a1, b1), our graphlet explanation for the Discussion class incorporates an additional edge and node, highlighted in green, compared to the ground truth motif proposed by GNNExplainer. This difference suggests that our graphlet explanation captures the presence of branch-out substructures, which are uniquely characteristic of Discussion graphs but not addressed by GNNExplainer’s motif. It is worth noting that the Discussion motif proposed by GNNExplainer (Fig. 5(a1)) is prevalent not only in typical Discussion graphs but also significantly in typical QA graphs. In Fig. 3(d1), although the graph represents a typical QA graph topology, a recurring pattern emerges where one of the two central nodes connects to three peripheral nodes. The fact that this recurring pattern in a representative QA graph is identified as the Discussion motif proposed by GNNExplainer (Fig. 5(a1)) underscores the limited explanatory power of their approach. In contrast, our explanations for the two classes (Fig. 5(b1, b2)) depict distinct topologies. As illustrated in Fig. 3(d1, d2), our Discussion explanation (Fig. 5(b1)) is not found in a typical QA graph (Fig. 3(d1)), while our QA explanation (Fig. 5(b2)) does not occur in a typical Discussion graph (Fig. 3(d2)). Moreover, our explanations are mutually exclusive, indicating that a 5-node connected subgraph classified as Fig. 5(b1) cannot be categorized as Fig. 5(b2) based on the edges among these 5 nodes. This highlights the unique substructures captured by our method. For the QA class, GNNExplainer proposed a recurring substructure as the QA motif (Fig. 5(a2)), which can be translated into an equivalent graphlet expression (Fig. 5(a3)). In contrast, GNNAnatomy directly captures the same substructure explanation (Fig. 5(b2)) in a systematic format, without the need for inference from recurring patterns. It is also crucial to recognize that merely presenting the topological traits of each class does not fully elucidate GNN’s behavior. As demonstrated in this study, different criteria apply to various groups of graphs. GNNAnatomy offers the flexibility to identify the groups and substructures that are most explanatory for the GNN’s behavior at specified granularities.

6.3 Study 2: MUTAG

Experiment settings. We train the GCN using the one-hot encoding of node degrees as the initial vector of each node, discarding any node and edge attributes provided in this dataset. Utilizing pure topological characteristics, the GCN model achieves a classification accuracy of 0.7667, while the surrogate model exhibits a cosine similarity of 0.7371 with the GCN probability output.

Group-level explanations. In molecular biology literature, certain substructures associated with mutagenicity have been identified, but there’s been limited discussion on non-mutagen-specific substructures. Thus, our study aims to extract traits used by GCN to classify a graph as mutagenic. In Fig. 6(a), we selected a group of graphs distributed diagonally and filtered out non-mutagens. This selection aims to identify structural differences (i.e., y-axis deviations) within the mutagenic graphs that contribute to disparities in graph embedding projections.

The top-ranked graphlets in factual explanation mode are both acyclic substructures: *graphlet₈* and *graphlet₂*, as shown in Fig. 6(b, c). In Fig. 6(b), a moderate negative correlation of -0.33 between

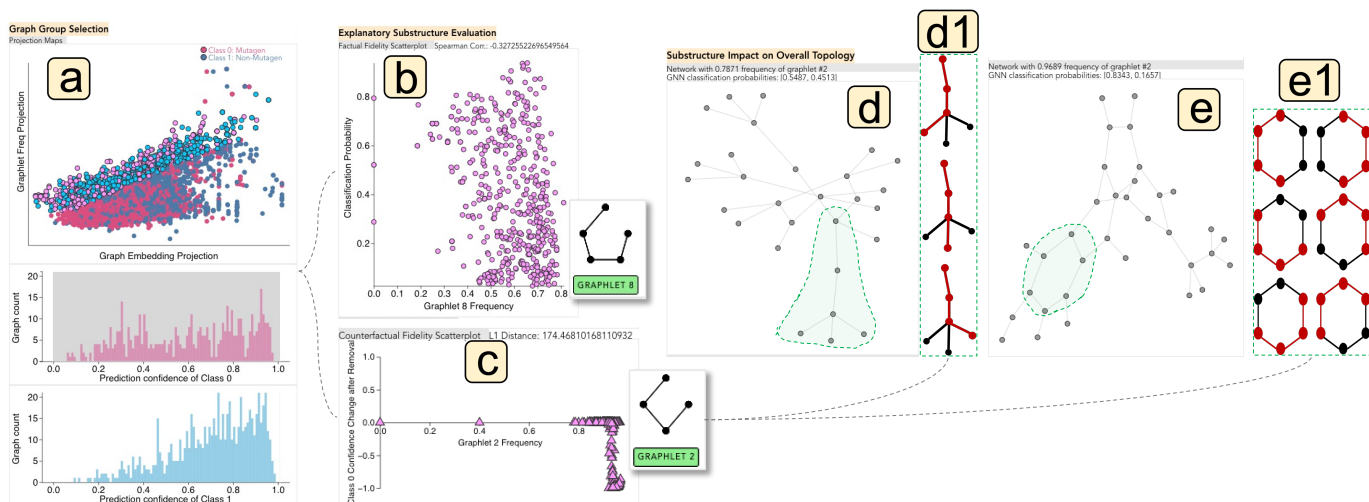


Fig. 6: (a) presents a selection of mutagenic graphs arranged diagonally, with the aim of identifying the mutagenic substructures that contribute the most to GCN classifications on the MUTAG dataset. In (b) and (c), we evaluate the validity of acyclic substructures $graphlet_8$ and $graphlet_2$, which are the top two relevant substructures ranked by our factual metric. (d) illustrates the typical structure of graphs with a lower frequency of $graphlet_2$, while (e) depicts the typical topology of graphs with a higher frequency of $graphlet_2$. We focus on the 6-node subgraphs in (d1) and (e1) to demonstrate that more acyclic patterns can be sampled from a ring than from a non-ring substructure (i.e., 3 vs. 6).

the frequency of $graphlet_8$ and classification probability indicates that a graph with a higher frequency of $graphlet_8$ has a higher chance of being classified as a mutagen. To investigate the necessity of the presence of these acyclic graphlets in classifying graphs as mutagens, we observe the impact on confidence scores from the removal of both $graphlet_2$ and $graphlet_8$. Due to the interdependency between $graphlet_2$ and $graphlet_8$, selecting to remove $graphlet_2$ automatically removes $graphlet_8$, as detailed in Sec. 4.4. In Fig. 6(c), the classification confidence scores decrease for a considerable number of graphs after the removal. This validates the necessity of $graphlet_2$ and $graphlet_8$, as GCN exhibits reduced confidence in classifying a graph as a mutagen when these substructures are absent from its topology.

Comparing Fig. 6(d) to Fig. 6(e), it is apparent that the presence of a 6-node ring structure is exclusive to the graph with a higher frequency of $graphlet_2$, indicating an association between the two. To validate this observation, we compare the number of $graphlet_2$ that can be sampled from a 6-node non-ring subgraph to that from a 6-node ring subgraph. As depicted in Fig. 6(d1, e1), we observe that a single ring structure can produce twice as many $graphlet_2$ as a non-ring structure can do. Furthermore, considering the edges attached to a ring structure, even more $graphlet_2$ can be sampled. Hence, the necessity of the presence of $graphlet_2$ and $graphlet_8$ in classifying graphs as mutagens by GCN may stem from the presence of a 6-node ring substructure.

In conclusion, every graph dataset may contain diverse topological traits that GNNs capture, which can be complex and unexpected. GNNAnatomy provides a systematic approach and ample visual aids to explore the fundamental substructure elements contributing to the significant structural traits associated with GNN classifications.

Qualitative evaluation. In Fig. 7(a1, a2, a3), GNNExplainer proposed three substructures commonly associated with mutagenicity: NO_2 , NH_2 , and the 6-atom carbon ring. However, as our methods focus on extracting pure structural importance, we do not directly compare our explanations with NO_2 and NH_2 , as they require node attributes to indicate their presence. Instead, we compare with the carbon ring, treated as a simple 6-node ring substructure. As summarized in Fig. 7(b1, b2), GNNAnatomy extracts two acyclic patterns as important topologies indicative of mutagenicity, which we infer from supporting visualizations to be incomplete rings, matching the proposed ground truth motif by GNNExplainer.

In summary, GNNAnatomy explores a diverse spectrum of substructures and uses visualizations to suggest any unexpected substructures that GNNs may utilize for classifications.

GNNExplainer		GNNAnatomy	
Mutagenic		Mutagenic	

Fig. 7: (a1, a2, a3) depict the ground truth motifs of the Mutagen class in the MUTAG dataset as proposed by GNNExplainer. (b1, b2) showcase the extracted explanatory graphlet substructures of mutagenicity by GNNAnatomy.

6.4 Study 3: BA-House

Experiment settings. The GCN is trained to classify whether a base graph generated by the Barabasi-Albert random graph model (BA) is attached with house motifs. The GCN model achieves a classification accuracy of 1.0, while the surrogate model shows a cosine similarity of 0.9421 with the GCN probability output.

Global-level explanations. Since the BA-House dataset is synthetic and the attached house motifs are known topological differences between the two classes, we aim to investigate if the GCN utilizes the house motif to distinguish graphs. We selected all 300 graphs to explore the global-level explanatory graphlets.

In Fig. 8(a), $graphlet_8$ is ranked first, indicating its relevance to the classification probability and its higher presence in House graphs. Additionally, in Fig. 8(a1), it shows that the frequency of $graphlet_8$ has a negative correlation (-0.4156) with the GCN classification probability. This suggests that a graph with a higher frequency of $graphlet_8$ has a larger chance of being classified as a House graph by the GCN. Moreover, in Fig. 8(a2), the confidence scores decrease for the House graphs but increase for Non-House graphs after the removal of $graphlet_8$, highlighting the necessity of its presence in classifying graphs as House graphs.

Investigating the influence of the house motif in Fig. 8(b), it is evident that Non-House graphs generally have a higher frequency of the house motif ($graphlet_{20}$) compared to graphs with attached house motifs. Additionally, as indicated in Fig. 8(b1), the frequency of $graphlet_{20}$ has a positive correlation (0.3828) with the GCN classification probability. This implies that a graph with a higher frequency of the house motif has a higher chance of being classified as, surprisingly, a Non-House graph by the GCN. Furthermore, as presented in Fig. 8(b2), the removal of the house motif counterintuitively increases the confidence scores for House graphs but decreases those for Non-House graphs.

Although the house motif indeed proves its relevance as per our hypothesis, its influence appears to be the exact opposite of what we

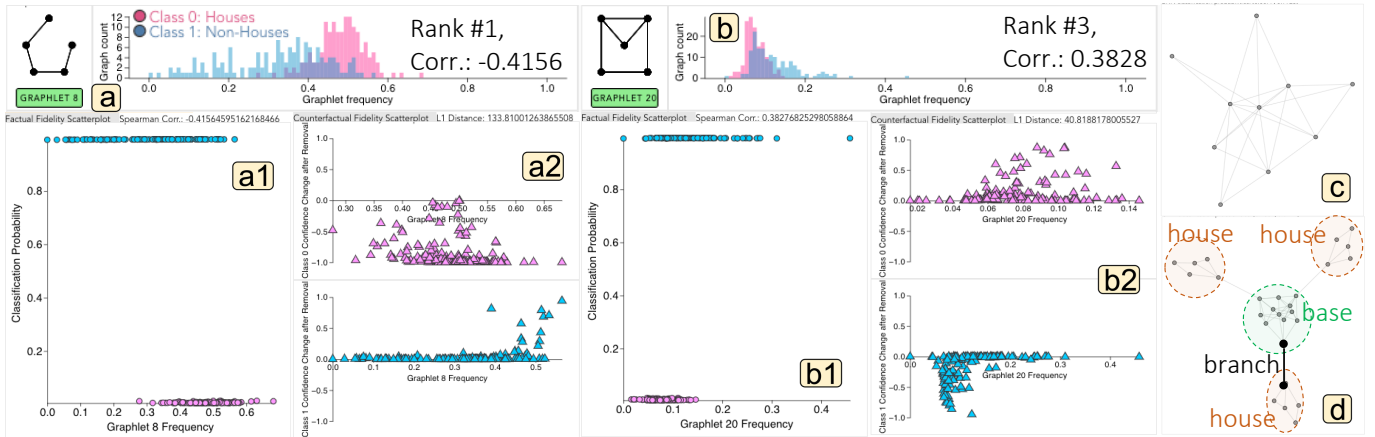


Fig. 8: In the BA-House dataset experiment, (a) illustrates the distribution of graphs based on the frequency of the house motif (i.e., $graphlet_{20}$), while (b) presents the distribution for $graphlet_8$. We observe opposite correlation signs in (a1) and (b1), along with opposite influences on the classification confidence scores of the two classes after removing the two substructures separately in (a2) and (b2). Further investigation in (c) and (d) reveals the root cause of this phenomenon: attaching house motifs to a BA base graph creates branch edges, as indicated in (d).

expected. To understand the causes, we examine the overall graph topologies. In Fig. 8(c), we observe that a BA-generated base graph (i.e., a Non-House graph) itself contains multiple house motifs due to its high connectivity among nodes. Conversely, a House graph, as shown in Fig. 8(d), has one node of each house motif attached to a node in the base graph, resulting in a lower overall edge density compared to a Non-House graph. As indicated in Fig. 8(d), the *branch* edges are the root cause of House graphs having a generally lower frequency of the house motif. Only one house motif could be sampled from each house attached. However, the *branch* edges connecting houses to the base graph allow the computation of graphlet frequency to sample additional 5-node connected subgraphs involving nodes in both the house and the base. These additional subgraph samples are not house motifs. For example, when 3 houses are attached, many more 5-node subgraphs can be sampled compared to a single base graph, but only 3 among those additional samples are house motifs. We validate our finding by computing the frequency of the house graphlet before and after attaching house motifs, which shows the average frequency indeed decreases from 0.1313 to 0.0686.

Upon further reasoning, we find that the *branch* edges may also contribute to $graphlet_8$ being the top-ranked explanatory substructure. As discussed, *branch* edges enable subgraph sampling across attached houses and the base graphs, increasing the chance of sampling an acyclic graphlet (i.e., $graphlet_8$). Conversely, due to the high connectivity of a Non-House graph, sampled 5-node subgraphs are rarely acyclic. In summary, despite our assumptions about what the GCN should utilize based on the known structural disparities, GNNAnatomy helps us identify the true decisive factors with ample evidence presented in the supporting visualizations. This study also paves the way for using our methods to validate presumed ground truth motifs for other synthetic graph datasets.

Qualitative evaluation. We posit that the graphlet sampling mechanism naturally leads to a higher frequency of acyclic substructures when attaching houses, but results in a lower frequency of the house graphlet. This raises the question of whether the graphlet sampling mechanism accurately reflects GNN behavior, warranting the connection of the results of the two.

Given that GNNs aggregate node information from direct neighbors in each layer, as explained in Sec. 2.2, they can capture a complete house motif within a 3-layer architecture. However, the presence of *branch* edges enables GNNs to aggregate information across both the base graph and the house motif, potentially hindering the GCN’s ability to fully capture a complete house topology in either component. This impact on neighbor sampling mirrors the discussion in this study concerning graphlet sampling. In essence, aggregating information within a Non-House graph encourages GNNs to sample neighboring nodes that collectively form complete house motifs. Therefore, using

graphlet distributions to depict the behavior of GNNs is indicative of their functioning.

7 DISCUSSION AND FUTURE WORKS

7.1 Scalability in Graphlet Frequency Computation

Using 3-, 4-, and 5-node graphlets ensures a diverse range of substructures while keeping the total number of graphlets manageable. For example, in a graph with 94 nodes and 222 edges, efficient sampling methods proposed in [23] yield 1106, 15113, and 172127 sampled 3-, 4-, and 5-node subgraphs, respectively. To compute the frequency of each graphlet for every graph, we iterate over these samples, checking for isomorphism with the target graphlet. Random sampling from this pool of subgraphs was attempted but found to compromise frequency precision. While this process may be time-consuming for larger networks, it is a one-time operation per dataset. The systematic generation and evaluation of explanations using graphlets justify the computational cost involved. To facilitate the more efficient use of GNNAnatomy with other datasets, we are working on developing a graphlet frequency benchmark dataset.

7.2 Generalizability

Other GNN models. GNNAnatomy operates as a post-hoc surrogate approach, leveraging graph embeddings and softmax probabilities generated by a trained GCN. This means that it can be applied to any GNN capable of producing a graph embedding for each graph, enabling explanations of its behavior across various levels of granularity.

Multi-class graph classification tasks. Even though we demonstrate GNNAnatomy’s capabilities using binary classification datasets, our approach can be expanded to multi-class classification tasks. Algorithmically, we need to change both factual and counterfactual metrics to computing the correlation and L1 distance for the chosen graphs within a single class. This adjustment will limit part of the versatility of GNNAnatomy, but can still allow systematic generation and evaluation of explanatory substructures.

Node classification tasks. While GNNAnatomy is primarily tailored for graph classification tasks, its methodology could potentially be adapted for explaining GNN behavior in node classification tasks as well. For instance, instead of utilizing graph embeddings and graph classification probabilities, we could employ node embeddings and node classification probabilities. Regarding graphlet frequency, we could substitute it with the frequency of a node appearing in a specific graphlet type, such as $graphlet_{20}$, relative to all occurrences of $graphlet_{20}$ found in the original graph. This approach would enable the identification of a node’s involvement in the overall graph topology within the context of graphlet representation.

Motifs with more than five nodes. As discussed in Sec. 6.3, the limitation of considering up to 5-node graphlets is that it cannot ex-

Explicitly capture motifs with more than 5 nodes. This limitation may arise when users expect certain large motifs to be utilized by GNNs. Instead of customizing the selection of graphlets to include these expected motifs, GNNAnatomy demonstrates the capability of implicitly capturing these motifs using fundamental substructure elements. With ample visualization support, GNNAnatomy assists users in formulating correct inferences about the explanatory motifs without the restriction of the number of nodes.

7.3 Extensibility

As discussed in Sec. 6.2, GCNs leverage different substructures to classify various groups of graphs. Specifically, we observe that GCNs utilize the branch-out substructure to distinguish graphs with distinct topologies. However, when there are no significant differences in graphlet distribution between classes, GCNs gradually resort to other suboptimal substructures (as seen in Fig. 4(b1)) to achieve satisfactory classifications. This observation suggests a potential extension of our work to develop a decision tree that hierarchically lists the substructure criteria employed by GCNs at each step for each group of graphs to attain the final performance. We intend to explore this application in future research.

8 CONCLUSION

We present a novel GNN explainer designed to facilitate systematic exploration and evaluation of diverse substructures that explain GNN behavior across multiple levels of granularity. Our approach leverages graphlets to generate substructure explanations and integrates factual and counterfactual reasoning logic to assess their validity. Interactive and supporting visualizations are incorporated to streamline the process of formulating a trustworthy explanation. Through case studies conducted on real-world and synthetic graph datasets spanning various domains, we demonstrate the efficacy of GNNAnatomy and compare the quality of our explanations to a state-of-the-art GNN explainer. While showcasing the versatility and utility of our approach, we outline future research directions for potential extensions of GNNAnatomy.

REFERENCES

- [1] M. Bajaj, L. Chu, Z. Y. Xue, J. Pei, L. Wang, P. C.-H. Lam, and Y. Zhang. Robust counterfactual explanations on graph neural networks. *Advances in Neural Information Processing Systems*, 34:5644–5655, 2021. 3
- [2] Z. Chen, F. Silvestri, J. Wang, Y. Zhang, Z. Huang, H. Ahn, and G. Tolomei. Grease: Generate factual and counterfactual explanations for gnn-based recommendations. *arXiv preprint arXiv:2208.04222*, 2022. 3
- [3] A. K. Debnath, R. L. Lopez de Compadre, G. Debnath, A. J. Shusterman, and C. Hansch. Structure-activity relationship of mutagenic aromatic and heteroaromatic nitro compounds. correlation with molecular orbital energies and hydrophobicity. *Journal of medicinal chemistry*, 34(2):786–797, 1991. 1, 6
- [4] K. Faust. A puzzle concerning triads in social networks: Graph constraints and the triad census. *Social Networks*, 32(3):221–233, 2010. 2
- [5] C. Frye, D. de Mijolla, T. Begley, L. Cowton, M. Stanley, and I. Feige. Shapley explainability on the data manifold. In *International Conference on Learning Representations*, 2020. 3
- [6] T. Funke, M. Khosla, and A. Anand. Hard masking for explaining graph neural networks. 2020. 2
- [7] G. Hooker and L. Mentch. Please stop permuting features: An explanation and alternatives. *arXiv preprint arXiv:1905.03151*, 2, 2019. 1, 3
- [8] S. Hooker, D. Erhan, P.-J. Kindermans, and B. Kim. A benchmark for interpretability methods in deep neural networks. *Advances in neural information processing systems*, 32, 2019. 1, 3
- [9] Q. Huang, M. Yamada, Y. Tian, D. Singh, and Y. Chang. Graphlime: Local interpretable model explanations for graph neural networks. *IEEE Transactions on Knowledge and Data Engineering*, 2022. 2
- [10] Z. Jin, Y. Wang, Q. Wang, Y. Ming, T. Ma, and H. Qu. Gnnlens: A visual analytics approach for prediction error diagnosis of graph neural networks. *IEEE Transactions on Visualization and Computer Graphics*, 2022. 3
- [11] T. N. Kipf and M. Welling. Semi-supervised classification with graph convolutional networks. *arXiv preprint arXiv:1609.02907*, 2016. 3
- [12] O. Kwon, T. Crnovrsanin, and K. Ma. What would a graph look like in this layout? A machine learning approach to large graph visualization. *IEEE Trans. Vis. Comput. Graph.*, 24(1):478–488, 2018. doi: 10.1109/TVCG.2017.2743858 2
- [13] B. La Rosa, G. Blasilli, R. Bourqui, D. Auber, G. Santucci, R. Capobianco, E. Bertini, R. Giot, and M. Angelini. State of the art of visual analytics for explainable deep learning. In *Computer Graphics Forum*, vol. 42, pp. 319–355. Wiley Online Library, 2023. 3
- [14] H. Li, X. Wang, Z. Zhang, and W. Zhu. Out-of-distribution generalization on graphs: A survey. *arXiv preprint arXiv:2202.07987*, 2022. 1, 3
- [15] Z. Liu, Y. Wang, J. Bernard, and T. Munzner. Visualizing graph neural networks with corgie: Corresponding a graph to its embedding. *IEEE Transactions on Visualization and Computer Graphics*, 28(6):2500–2516, 2022. 3
- [16] A. Lucic, M. A. Ter Hoeve, G. Tolomei, M. De Rijke, and F. Silvestri. CF-GNNexplainer: Counterfactual explanations for graph neural networks. In *International Conference on Artificial Intelligence and Statistics*, pp. 4499–4511. PMLR, 2022. 3
- [17] D. Luo, W. Cheng, D. Xu, W. Yu, B. Zong, H. Chen, and X. Zhang. Parameterized explainer for graph neural network. *Advances in neural information processing systems*, 33:19620–19631, 2020. 1, 2
- [18] S. Miao, M. Liu, and P. Li. Interpretable and generalizable graph learning via stochastic attention mechanism. In *International Conference on Machine Learning*, pp. 15524–15543. PMLR, 2022. 1, 3
- [19] P. E. Pope, S. Kolouri, M. Rostami, C. E. Martin, and H. Hoffmann. Explainability methods for graph convolutional neural networks. In *Proceedings of the IEEE/CVF conference on computer vision and pattern recognition*, pp. 10772–10781, 2019. 1, 3
- [20] N. Pržulj. Biological network comparison using graphlet degree distribution. *Bioinformatics*, 23(2):e177–e183, 2007. 2
- [21] B. Sanchez-Lengeling, J. Wei, B. Lee, E. Reif, P. Wang, W. Qian, K. McCloskey, L. Colwell, and A. Wiltchko. Evaluating attribution for graph neural networks. *Advances in neural information processing systems*, 33:5898–5910, 2020. 3
- [22] M. S. Schlichtkrull, N. D. Cao, and I. Titov. Interpreting graph neural networks for [nlp] with differentiable edge masking. In *International Conference on Learning Representations*, 2021. 2, 3
- [23] N. Shervashidze, S. Vishwanathan, T. Petri, K. Mehlhorn, and K. Borgwardt. Efficient graphlet kernels for large graph comparison. In *Artificial intelligence and statistics*, pp. 488–495. PMLR, 2009. 2, 3, 9
- [24] J. Tan, S. Geng, Z. Fu, Y. Ge, S. Xu, Y. Li, and Y. Zhang. Learning and evaluating graph neural network explanations based on counterfactual and factual reasoning. In *Proceedings of the ACM Web Conference 2022*, pp. 1018–1027, 2022. 3
- [25] J. Ugander, L. Backstrom, and J. Kleinberg. Subgraph frequencies: Mapping the empirical and extremal geography of large graph collections. In *Proceedings of the International Conference on World Wide Web*, p. 1307–1318, 2013. 2
- [26] M. Vu and M. T. Thai. Pgm-explainer: Probabilistic graphical model explanations for graph neural networks. *Advances in neural information processing systems*, 33:12225–12235, 2020. 1, 2
- [27] Q. Wang, K. Huang, P. Chandak, M. Zitnik, and N. Gehlenborg. Extending the nested model for user-centric xai: A design study on gnn-based drug repurposing. *IEEE Transactions on Visualization and Computer Graphics*, 29(1):1266–1276, 2022. 1, 3
- [28] X. Wang, Y. Wu, A. Zhang, X. He, and T.-s. Chua. Causal screening to interpret graph neural networks. 2020. 2
- [29] Y.-X. Wu, X. Wang, A. Zhang, X. He, and T.-S. Chua. Discovering invariant rationales for graph neural networks. *arXiv preprint arXiv:2201.12872*, 2022. 1, 3
- [30] Y.-X. Wu, X. Wang, A. Zhang, X. Hu, F. Feng, X. He, and T.-S. Chua. Deconfounding to explanation evaluation in graph neural networks. *arXiv preprint arXiv:2201.08802*, 2022. 3
- [31] H. Xuanyuan, P. Barbiero, D. Georgiev, L. C. Magister, and P. Liò. Global concept-based interpretability for graph neural networks via neuron analysis. In *Proceedings of the AAAI Conference on Artificial Intelligence*, vol. 37, pp. 10675–10683, 2023. 1, 2
- [32] P. Yanardag and S. Vishwanathan. Deep graph kernels. In *Proceedings of the 21th ACM SIGKDD international conference on knowledge discovery and data mining*, pp. 1365–1374, 2015. 6
- [33] Z. Ying, D. Bourgeois, J. You, M. Zitnik, and J. Leskovec. GNNExplainer: Generating explanations for graph neural networks. *Advances in neural information processing systems*, 32, 2019. 1, 2, 3, 6
- [34] Z. Yu and H. Gao. Motifexplainer: a motif-based graph neural network explainer. *arXiv preprint arXiv:2202.00519*, 2022. 2

- [35] H. Yuan, J. Tang, X. Hu, and S. Ji. Xgnn: Towards model-level explanations of graph neural networks. In *Proceedings of the 26th ACM SIGKDD International Conference on Knowledge Discovery & Data Mining*, pp. 430–438, 2020. [1](#), [2](#)
- [36] H. Yuan, H. Yu, S. Gui, and S. Ji. Explainability in graph neural networks: A taxonomic survey. *IEEE Transactions on Pattern Analysis and Machine Intelligence*, 2022. [1](#), [2](#)
- [37] H. Yuan, H. Yu, J. Wang, K. Li, and S. Ji. On explainability of graph neural networks via subgraph explorations. In *International conference on machine learning*, pp. 12241–12252. PMLR, 2021. [2](#)
- [38] Y. Zhang, D. Defazio, and A. Ramesh. Relax: A model-agnostic relational model explainer. In *Proceedings of the 2021 AAAI/ACM Conference on AI, Ethics, and Society*, pp. 1042–1049, 2021. [2](#)